Applied Physics Letters

RESEARCH ARTICLE | JANUARY 21 2025

Investigation of the $4f^{14}6s^{2}\,{}^{1}S_{0}$–$4f^{13}5d6s^{2}$ ($J = 2$) clock transition at 431 nm of ^{171}Yb atoms trapped in an optical lattice

Congyu Wang ; Yuan Yao ; Haosen Shi ; Hongfu Yu ; Longsheng Ma ; Yanyi Jiang

Appl. Phys. Lett. 126, 031101 (2025)
https://doi.org/10.1063/5.0246836

Applied Physics Letters ARTICLE pubs.aip.org/aip/apl

Investigation of the $4f^{14}6s^2\ ^1S_0-4f^{13}5d6s^2$ ($J=2$) clock transition at 431 nm of ^{171}Yb atoms trapped in an optical lattice

Cite as: Appl. Phys. Lett. **126**, 031101 (2025); doi: 10.1063/5.0246836
Submitted: 4 November 2024 · Accepted: 7 January 2025 ·
Published Online: 21 January 2025

View Online Export Citation CrossMark

Congyu Wang,[1] Yuan Yao,[1,a)] Haosen Shi,[1] Hongfu Yu,[1] Longsheng Ma,[1,2] and Yanyi Jiang[1,2,a)]

AFFILIATIONS

[1]State Key Laboratory of Precision Spectroscopy, East China Normal University, Shanghai 200062, China
[2]Collaborative Innovation Center of Extreme Optics, Shanxi University, Taiyuan 030006, China

[a)]Authors to whom correspondence should be addressed: yyao@lps.ecnu.edu.cn and yyjiang@phy.ecnu.edu.cn

ABSTRACT

With the aid of an optical frequency divider based on an optical frequency comb, the frequency of a laser at 431 nm is divided from a cavity-stabilized laser at 578 nm. Using the frequency-stabilized 431 nm laser, we observe a 2.5 kHz linewidth $4f^{14}6s^2\ ^1S_0-4f^{13}5d6s^2$ ($J=2$) transition of ^{171}Yb atoms trapped in an optical lattice. By measuring the lattice-induced frequency shift, we determine the magic wavelength of the optical lattice for the 431 nm transition to be 797.97(20) nm. The frequency of the 431 nm transition is measured to be 695 171 054 856.9(1.1) kHz by referencing to the $^1S_0-^3P_0$ transition at 578 nm of Yb atoms.

Recently, precision spectroscopy of ytterbium (Yb) has drawn wide attention. Optical clocks based on the $^1S_0-^3P_0$ transition of ^{171}Yb atoms at 578 nm demonstrate their extraordinary performance in a frequency instability of $1.5\times10^{-16}/\sqrt{\tau}$ and a frequency uncertainty of 1.4×10^{-18}.[1] They support frequency ratio measurement against other optical atomic clocks with uncertainties at the 10^{-18} level.[2] Optical clocks based on the $^2S_{1/2}$ ($F=0$)$-^2F_{7/2}$ ($F=3$) electric octupole transition at 467 nm of a single trapped Yb^+ have similar uncertainties of 3×10^{-18}.[3] Such precise and accurate optical clocks play a critical role in the redefinition of the International System of Units (SI) second and precision measurements such as tests of fundamental physics, geodesy, and the search for dark matter.[1–8] By measuring isotope shifts of laser cooled and trapped neutral Yb atoms or Yb ions, new forces beyond the standard model have been searched.[9–11] Moreover, by comparing two narrow-linewidth transitions (electric quadrupole at 436 nm and electric octupole at 467 nm) of a single trapped Yb^+ over time, temporal variation of the fine structure constant is improved to $1.0(1.1)\times10^{-18}$/yr.[6]

The $^1S_0-^3P_2$ transition of neutral Yb atoms at 507 nm has rarely been studied, mostly due to its similarity to the well-known 578 nm clock transition.[12] A third long-lived excited state of $4f^{13}5d6s^2$ ($J=2$) has been introduced for its lower blackbody radiation-induced frequency shift at room temperature ($\sim6\times$ smaller compared to the 578 nm transition) and a high sensitivity to the fine structure constant variation.[13–15] To connect with this state, Yb atoms can be excited from the $^1S_0$, $^3P_0$, or $^3P_2$ state, corresponding to a wavelength of 431, 1695, and 2875 nm, respectively. The relative energy levels and transitions are as shown in Fig. 1.

Ishiyama *et al.* were the first to observe the transitions to the $4f^{13}5d6s^2$ ($J=2$) state.[16] They observe Doppler broadening-limited 30 kHz linewidth spectra at 431 nm for all the isotopes of Yb atoms trapped in a crossed far-off resonance trap and a 12 kHz-linewidth spectrum for lattice-trapped ^{174}Yb atoms. Later, the absolute frequency of the $^1S_0$ ($F=1/2$)$-4f^{13}5d6s^2$ ($J=2$, $F=3/2$) transition at 431 nm of ^{171}Yb trapped in a magneto-optical trap (MOT) was determined to be 695 171 054 858.1(8.2) kHz by comparing against physical realization of Coordinated Universal Time. The measurement uncertainty includes a statistical uncertainty of 3.25 kHz and a systematic uncertainty of 7.65 kHz dominated by the AC Stark shift of the MOT laser.[17] Later, the absolute frequency of the transition for other isotopes of Yb were also measured with an uncertainty of $\sim$10 kHz.[18] To obtain an observed spectral linewidth unlimited by Doppler broadening, Qiao *et al.* loaded ^{171}Yb atoms into an optical lattice close to its magic wavelength and observed a 4 kHz linewidth spectrum of the $^3P_0$ ($F=1/2$) $-4f^{13}5d6s^2$ ($J=2$, $F=3/2$) transition (1695 nm).[19] With the aid of an optical frequency comb and a hydrogen maser calibrated by the Yb optical clock, they also measured the transition frequency with an uncertainty of 1.3 kHz, which is dominated by the frequency shift due to fiber transmission and lattice light.

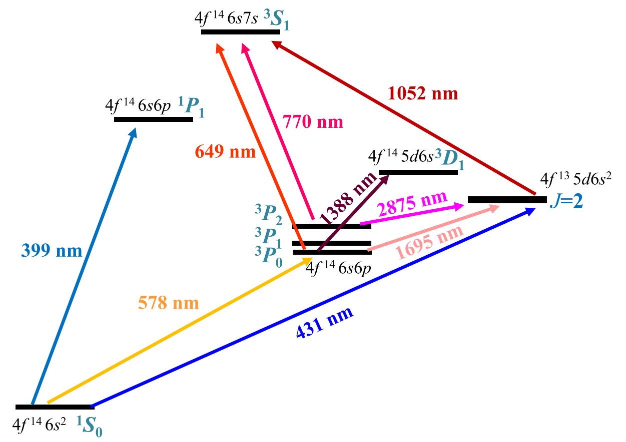

FIG. 1. The relevant energy levels and transitions for ^{171}Yb atoms.

In this paper, we trap laser-cooled ^{171}Yb atoms into an optical lattice. To excite the 431 nm transition, using an optical frequency divider we stabilize the 431 nm laser frequency by referencing its fundamental laser at 862 nm to a cavity-stabilized laser at 578 nm.[20,21] The frequency of the 578 nm laser is calibrated by the $^1S_0{-}^3P_0$ transition of ^{171}Yb atoms. A Rabi spectrum of the $^1S_0$ ($F = 1/2$)$-4f^{13}5d6s^2$ ($J = 2$, $F = 3/2$) transition is observed with a linewidth of 2.5 kHz, corresponding to a quality factor of $Q \sim 2.8 \times 10^{11}$. The frequency shift of the transition due to the lattice light is investigated, yielding a magic wavelength of 797.97(20) nm when the polarization of the lattice light is aligned perpendicular to the quantization axis. By setting the lattice light frequency close to the magic wavelength and averaging two $m_F = \pm 1/2$ transitions to cancel the first Zeeman shift, the frequency of the transition is measured to be 695 171 054 856.9 kHz with an uncertainty of 1.1 kHz dominated by lattice light shift and statistical noise.

The schematic diagram of our experiment is shown in Fig. 2(a). The details of laser cooling and trapping of Yb atoms can be found in Ref. 22. After a two-stage MOT, the ^{171}Yb atoms are loaded into a one-dimensional optical lattice at about 798 nm, generated from a single frequency, continuous wave Ti:sapphire laser. As much as a 600 mW laser light is delivered to the apparatus using a piece of polarization maintenance (PM) optical fiber. The power of the lattice light is monitored on a photo detector (PD$_1$). The optical lattice is formed by a focused beam, which is then retro-reflected by a curved mirror. The optical lattice is tilted from the vertical axis by about 5°. The operating trap depth of the lattice is $\sim 100E_r$ with $E_r = (h\nu_{lat})^2/(2m_{Yb} \times c^2)$, where h *is* the Planck constant, ν_{lat} is the lattice frequency, m_{Yb} is the mass of ^{171}Yb atom, and c is the speed of light. The diameter of the optical lattice is about 110 μm. Nearly 10^4 ^{171}Yb atoms are trapped in the optical lattice.

The probe laser light at 431 nm (from Precilasers) is the second harmonic of an 862 nm laser, which is summed from a diode laser at 1952.8 nm and a fiber laser at 1544.8 nm. As shown in Fig. 2(b), part of the 862 nm laser is sent to an optical frequency divider based on an optical frequency comb.[20,21,23] The optical frequency divider sets the frequency ratio between a reference laser at 578 nm and the 862 nm laser as $\nu_{862} = \nu_{Yb}/R_x$, where R_x is the preset frequency divisor of the optical frequency divider determined by the settings of direct digital synthesizers (DDSs). The reference laser is a cavity-stabilized laser at 578 nm, which is calibrated by the $^1S_0{-}^3P_0$ transition of a second ensemble of ^{171}Yb atoms. The frequency uncertainty of the $^1S_0{-}^3P_0$ transition is below 1 Hz. Here, we denote the frequency of the reference laser as ν_{Yb}. The optical frequency comb is frequency-stabilized to a hydrogen maser, which means both f_r and f_0 are phase-locked to signals synthesized from the maser. The comb frequency noise onto the 862 nm laser is eliminated with the transfer oscillator scheme.[24] In brief, we use mixers and DDSs to remove the carrier-envelope offset frequency (f_0) and repetition rate (f_r) of the comb from the beat notes between ν_{862} (ν_{Yb}) and their nearby comb teeth.[20,21,23] As a result, a virtual beat note between ν_{862} and ν_{Yb} is obtained, which is free of f_0 and f_r. Then this signal is sent to a servo for stabilizing the frequency of the 862 nm laser by feedbacking to the current of the 1952.8 nm laser (fast) and to a piezo inside the 1544.8 nm laser (slow). The servo bandwidth of the 862 nm laser is about 150 kHz. During the detection of the 431 nm transition, we scan ν_{862} by adjusting the divisor of the optical frequency divider (see Refs. 20 and 23 for more experimental details of the optical frequency divider). We use optical fibers to transfer the 862 and 431 nm laser light to the optical frequency divider and the apparatus of the lattice-trapped Yb atoms, where fiber-induced random phase noise is not compensated in this work. We test the fiber

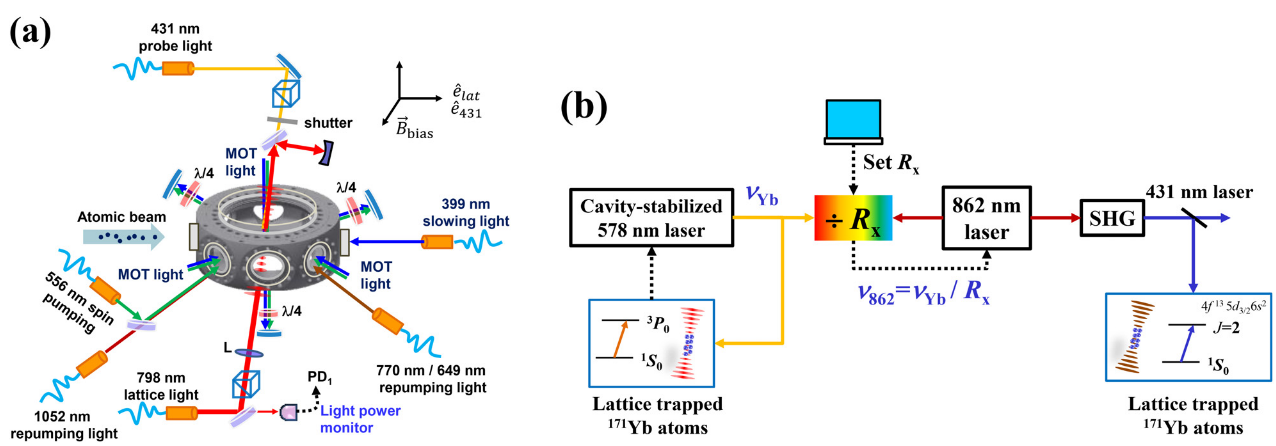

FIG. 2. Schematic diagram of the experimental setup. (a) Laser cooling, trapping, and probing of ^{171}Yb atoms. (b) Frequency stabilization of the 431 nm laser.

noise-induced laser linewidth to be <200 Hz and the fiber noise-induced laser frequency instability to be $<2\times10^{-15}$ at 1 s averaging time. The observed spectra in the following text are not limited by the 431 nm laser.

We use the frequency-controlled 431 nm laser to probe the ^{171}Yb atoms trapped in the optical lattice. A magnetic field $\vec{B}_{\text{bias}}$ is applied to split the Zeeman sub-levels. The polarization of the lattice light $\hat{e}_{\text{lat}}$ is perpendicular to the quantization axis. Before interrogation with the 431 nm laser, the atoms are prepared in one of the spin states $|^1S_0, m_F = \pm1/2\rangle$ with a 556 nm laser light. Rabi interrogation is performed by applying the 431 nm probe light with a power of 1.7 mW and a diameter of about 2 mm to excite the $^1S_0$ $(F = 1/2)$–$4f^{13}5d6s^2$ $(J = 2, F = 3/2)$ transition. The polarization of the 431 nm probe light is aligned along $\hat{e}_{\text{lat}}$. In each frequency sweep step, the populations in the ground and excited states are separately measured using the shelving detection technique. The population in the ground state is measured by exciting the atoms to the $^1P_1$ state with a pulse of 399 nm laser light and detecting the fluorescence when the atoms decay back to the ground state. In measuring the population of the atoms in the excited state, the atoms are repumped back to the ground state via the channels of $4f^{13}5d6s^2$ $(J = 2) \rightarrow {}^3S_1$, ${}^3P_0 \rightarrow {}^3S_1$, and ${}^3P_2 \rightarrow {}^3S_1$. Then, we measure the population of the atoms repumped to the ground state using the above-mentioned method. All the repumping laser light are shone on the atoms for 5 ms. The efficiency of this combination of repumping can reach more than 90%.

With an interrogation time of 200 ms, Rabi spectra with a linewidth of 2.5 kHz is obtained, as shown in Fig. 3(a). Such a spectrum corresponds to a quality factor of $Q \sim 2.8\times10^{11}$. The maximum excited rate is 0.3. The linewidth of these two spectra cannot be further reduced by increasing the probe time or reducing the power of the probe light. We attribute it to residual magnetic noise. Such a problem does not happen to the traditional 578 nm clock transition of Yb atoms at an observed spectral linewidth of ∼1 Hz since the $^3P_0$ state is nearly four orders of magnitude less sensitive to magnetic field compared to the $4f^{13}5d6s^2$ $(J = 2)$ state.[14,19]

We investigate the lattice-induced frequency shift of the 431 nm transition by measuring the average frequency of two π transitions as those shown in Fig. 3(a) under two lattice trap depths of $72E_r$ and $144E_r$ in an interleave mode. Figure 3(b) shows the lattice-induced frequency shift of the 431 nm transition at different lattice frequencies. Each error bar is dominated by the statistical uncertainty of the frequency shift. With the aid of a dispersion fit curve, the magic wavelength is determined to be $\lambda_L = 797.97(20)$ nm when $\Delta\nu(\lambda_L) = 0$, only 0.7 nm away from that predicted in Ref. 16. With this measurement, we can obtain the lattice-induced frequency shift of the 431 nm transition to be -0.09 ± 0.85 kHz at a lattice trap depth of $100E_r$ in the following frequency measurement.

We also measure the absolute frequency by averaging the two π transitions using the optical frequency divider shown in Fig. 2(b). Table I shows the uncertainty budget for the absolute frequency measurement. The AC Stark shift induced by the probe light is evaluated by measuring the frequency shift when the power of the probe light is separately set to $P_0 = 1.7$ mW and $P_1 = 12$ mW. The frequency shift is measured to be 0.4 ± 0.7 kHz. Therefore, we determine that the AC Stark shift due to the probe light is 0.07(11) kHz at $P_0 = 1.7$ mW. The measurement uncertainty of the probe light-induced frequency shift covers the theoretical result from Ref. 14. The first-order Zeeman shift

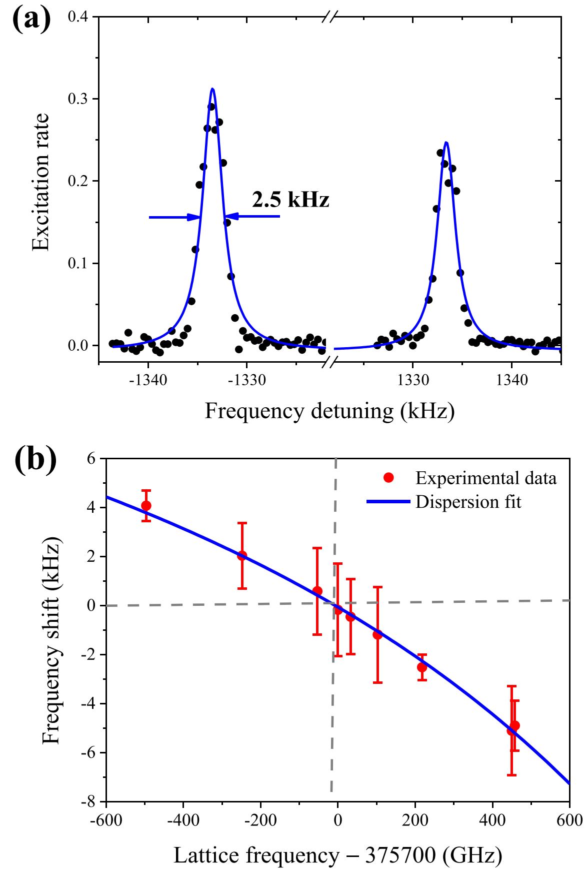

FIG. 3. Experimental results. (a) A spectrum of the $|^1S_0, m_F = \pm1/2\rangle \rightarrow |4f^{13}5d6s^2 (J = 2), F = 3/2, m_F = \pm1/2\rangle$ transition with a bias magnetic field applied. (b) Lattice light-induced frequency shift of the 431 nm transition at a trap depth of $100E_r$ as a function of lattice frequency. The frequency shift crosses zero when the lattice frequency is close to 375.696(92) THz, corresponding to a magic wavelength of 797.97(20) nm.

is canceled by averaging the two π transitions. We use the frequency splitting of the two π transitions to determine the applied bias magnetic field with the first-order Zeeman shift coefficient of 2.44(5) MHz/G/m_F.[19] Then we use the coefficient of -358 Hz/G^2 to determine

TABLE I. Systematic frequency shifts and uncertainties for frequency measurement of the $^1S_0$ $(F = 1/2)$–$4f^{13}5d6s^2$ $(J = 2, F = 3/2)$ transition.

	Frequency shift (kHz)	Uncertainty (kHz)
Lattice light	−0.09	0.85
Probe light	0.07	0.11
Second-order Zeeman	−0.43	0.02
Frequency measurement	0	0.03
Other effects	0	<0.01
Statistical	0	0.61
Total	**−0.45**	**1.1**

the second-order Zeeman shift to be −0.43(2) kHz. The second-order Zeeman shift coefficient is calculated with Eq. (7) from Ref. 25. The frequency of the cavity-stabilized laser at 578 nm is calibrated before and after the frequency measurement of the 431 nm transition. The frequency measurement uncertainty, including the frequency drift of the 578 nm reference laser, uncompensated fiber-induced laser frequency noise, and the optical frequency divider, is estimated to be 30 Hz. Other effects, such as blackbody radiation, higher-order lattice light shift, atomic collision, and DC Stark shift, are negligible, which is estimated using the 578 nm clock transition with the same apparatus. The coefficient of the blackbody radiation shift is from Refs. 13–17.

In the experiment, using the optical frequency divider, we directly obtain the frequency ratio between the frequency-calibrated 578 nm laser and the 431 nm transition from the settings of the DDSs. The time base of a tunable DDS is an optically divided RF signal at ∼10 MHz, whose frequency is $f_{\mathrm{time}} = \nu_{\mathrm{Yb}}/K$, where K is a divisor determined by DDSs.[20,21,23] After correcting the above frequency shift, the frequency ratio between the two clock transitions is $\nu_{431}/\nu_{578} = 1.341\,263\,050\,519(2)$. Then, we use the frequency ratio to calculate the frequency of the $^1S_0$ $(F = 1/2)$–$4f^{13}5d6s^2$ $(J = 2, F = 3/2)$ transition to be 695 171 054 856.9(1.1) kHz, which agrees with Ref. 17.

In summary, we observe a 2.5 kHz linewidth Rabi spectrum of the $^1S_0$ $(F = 1/2)$–$4f^{13}5d6s^2$ $(J = 2, F = 3/2)$ transition. The magic wavelength for the lattice laser is determined to be 797.97(20) nm when the polarization of the lattice light is aligned perpendicular to the quantization axis. The frequency of the transition is determined to be 695 171 054 856.9(1.1) kHz, dominated by lattice light shift measurement. Further reduction in spectral linewidth will help even more precise frequency measurement, which is critical for the development of optical atomic clocks and the search for new physics. Since residual magnetic noise might be the main cause of the broadened spectra, one path to obtain a narrower spectral linewidth is to reduce the magnetic field noise. A magnetic field shielding and a low noise current source for the bias magnetic field are expected to reduce the magnetic field noise by about an order of magnitude. For another, since the 431 nm transition for bosons has less Zeeman shift, in the next step we will also try to explore it.

This work was supported by the National Natural Science Foundation of China (Grant Nos. 11927810, 12334020, and 12341404) and the National Key R&D Program of China (Grant No. 2022YFB3904001). We are grateful to Z. M. Tang and Y. Yang from Fudan University for useful discussion.

AUTHOR DECLARATIONS

Conflict of Interest

The authors have no conflicts to disclose.

Author Contributions

Congyu Wang: Data curation (equal); Formal analysis (equal); Writing – review & editing (equal). **Yuan Yao:** Conceptualization (equal); Data curation (equal); Formal analysis (equal); Funding acquisition (equal); Resources (equal); Writing – review & editing (equal). **Haosen Shi:** Resources (equal); Writing – review & editing (equal). **Hongfu Yu:** Resources (equal). **Longsheng Ma:** Conceptualization (equal); Funding acquisition (equal); Writing – review & editing (equal). **Yanyi Jiang:** Conceptualization (equal); Data curation (equal); Formal analysis (equal); Funding acquisition (equal); Supervision (equal); Writing – original draft (equal); Writing – review & editing (equal).

DATA AVAILABILITY

The data that support the findings of this study are available from the corresponding authors upon reasonable request.

REFERENCES

1. W. F. McGrew, X. Zhang, R. J. Fasano, S. A. Schäffer, K. Beloy, D. Nicolodi, R. C. Brown, N. Hinkley, G. Milani, M. Schioppo, T. H. Yoon, and A. D. Ludlow, "Atomic clock performance enabling geodesy below the centimetre level," Nature **564**, 87 (2018).
2. K. Beloy, M. I. Bodine, T. Bothwell, S. M. Brewer, S. L. Bromley, J.-S. Chen, J.-D. Deschênes, S. A. Diddams, R. J. Fasano, T. M. Fortier *et al.*, "Frequency ratio measurements at 18-digit accuracy using an optical clock network," Nature **591**, 564 (2021).
3. N. Huntemann, C. Sanner, B. Lipphardt, C. Tamm, and E. Peik, "Single-ion atomic clock with 3×10^{-18} systematic uncertainty," Phys. Rev. Lett. **116**, 063001 (2016).
4. F. Riehle, P. Gill, F. Arias, and L. Robertsson, "The CIPM list of recommended frequency standard values: Guidelines and procedures," Metrologia **55**, 188 (2018).
5. C. Sanner, N. Huntemann, R. Lange, C. Tamm, E. Peik, M. S. Safronova, and S. G. Porsev, "Optical clock comparison for Lorentz symmetry testing," Nature **567**, 204 (2019).
6. R. Lange, N. Huntemann, J. M. Rahm, C. Sanner, H. Shao, B. Lipphardt, C. Tamm, S. Weyers, and E. Peik, "Improved limits for violations of local position invariance from atomic clock comparisons," Phys. Rev. Lett. **126**, 011102 (2021).
7. M. Takamoto, I. Ushijima, N. Ohmae, T. Yahagi, K. Kokado, H. Shinkai, and H. Katori, "Test of general relativity by a pair of transportable optical lattice clocks," Nat. Photonics **14**, 411 (2020).
8. M. Filzinger, S. Dörscher, R. Lange, J. Klose, M. Steinel, E. Benkler, E. Peik, C. Lisdat, and N. Huntemann, "Improved limits on the coupling of ultralight bosonic dark matter to photons from optical atomic clock comparisons," Phys. Rev. Lett. **130**, 253001 (2023).
9. J. Hur, D. P. L. Aude Craik, I. Counts, E. Knyazev, L. Caldwell, C. Leung, S. Pandey, J. C. Berengut, A. Geddes, W. Nazarewicz, P.-G. Reinhard, A. Kawasaki, H. Jeon, W. Jhe, and V. Vuletić, "Evidence of two-source king plot nonlinearity in spectroscopic search for new boson," Phys. Rev. Lett. **128**, 163201 (2022).
10. N. L. Figueroa, J. C. Berengut, V. A. Dzuba, V. V. Flambaum, D. Budker, and D. Antypas, "Precision determination of isotope shifts in ytterbium and implications for new physics," Phys. Rev. Lett. **128**, 073001 (2022).
11. K. Ono, Y. Saito, T. Ishiyama, T. Higomoto, T. Takano, Y. Takasu, Y. Yamamoto, M. Tanaka, and Y. Takahashi, "Observation of nonlinearity of generalized king plot in the search for new boson," Phys. Rev. X **12**, 021033 (2022).
12. Y. Sakamoto, Y. Kawai, D. Akamatsu, and F.-L. Hong, "Precision spectroscopy of iodine absorption lines near the $^1S_0$-$^3P_2$ transition of Yb atoms at 507 nm," Jpn. J. Appl. Phys., Part 1 **63**, 032006 (2024).
13. M. S. Safronova, S. G. Porsev, C. Sanner, and J. Ye, "Two clock transitions in neutral Yb for the highest sensitivity to variations of the fine-structure constant," Phys. Rev. Lett. **120**, 173001 (2018).
14. V. A. Dzuba, V. V. Flambaum, and S. Schiller, "Testing physics beyond the standard model through additional clock transitions in neutral ytterbium," Phys. Rev. A **98**, 022501 (2018).
15. Z.-M. Tang, Y. Yu, B. K. Sahoo, C.-Z. Dong, Y. Yang, and Y. Zou, "Simultaneous magic trapping conditions for three additional clock transitions in Yb to search for variation of the fine-structure constant," Phys. Rev. A **107**, 053111 (2023).
16. T. Ishiyama, K. Ono, T. Takano, A. Sunaga, and Y. Takahashi, "Observation of an inner-shell orbital clock transition in neutral ytterbium atoms," Phys. Rev. Lett. **130**, 153402 (2023).

[17] A. Kawasaki, T. Kobayashi, A. Nishiyama, T. Tanabe, and M. Yasuda, "Observation of the 4f ^{14}6s^2 ^{1}S$_0$–4f ^{13}5d6s^2 (J = 2) clock transition at 431 nm in ^{171}Yb," Phys. Rev. A **107**, L060801 (2023).
[18] A. Kawasaki, T. Kobayashi, A. Nishiyama, T. Tanabe, and M. Yasuda, "Isotope-shift analysis with the 4f ^{14}6s^2 ^{1}S$_0$–4f ^{13}5d6s^2 (J = 2) transition in ytterbium," Phys. Rev. A **109**, 062806 (2024).
[19] H. Qiao, D. Ai, C.-Y. Sun, C.-Q. Peng, Q.-C. Qi, C.-C. Zhao, L.-M. Luo, T.-Y. Jin, T. Zhang, M. Zhou, and X.-Y. Xu, "Investigation of the 6s6p ^{3}P$_0$–4f ^{13}5d6s^2 (J = 2) clock transition in ^{171}Yb atoms," Phys. Rev. X **14**, 011023 (2024).
[20] Y. Yao, Y. Jiang, H. Yu, Z. Bi, and L. Ma, "Optical frequency divider with division uncertainty at the 10^{-21} level," Natl. Sci. Rev. **3**, 463 (2016).
[21] H. Shi, Y. Jiang, Y. Yao, B. Li, C. Wang, H. Yu, and L. Ma, "Optical frequency divider: Capable of measuring optical frequency ratio in 22 digits," APL Photonics **8**, 100802 (2023).
[22] Y. Sun, Y. Yao, Y. Hao, H. Yu, Y. Jiang, and L. Ma, "Laser stabilizing to ytterbium clock transition with Rabi and Ramsey spectroscopy," Chin. Opt. Lett. **18**, 070201 (2020).
[23] Y. Yao, H. Shi, G. Yang, B. Li, C. Wang, H. Yu, L. Ma, and Y. Jiang, "Coherent link between a Ti: Sapphire comb and a 1.5 μm laser via nonlinear interaction in photonic crystal fiber," Photonics Res. **12**, 350 (2024).
[24] H. R. Telle, B. Lipphardt, and J. Stenger, "Kerr-lens, mode-locked lasers as transfer oscillators for optical frequency measurements," Appl. Phys. B **74**, 1 (2002).
[25] A. A. Golovizin, D. O. Tregubov, E. S. Fedorova, D. A. Mishin, D. I. Provorchenko, K. Y. Khabarova, V. N. Sorokin, and N. N. Kolachevsky, "Simultaneous bicolor interrogation in thulium optical clock providing very low systematic frequency shifts," Nat. Commun. **12**, 5171 (2021).